Submitted to Journal of Molecular Spectroscopy

LBL-2590
Preprint c.2

MICROWAVE SPECTRUM OF SILYL METHYL ETHER

Charles D. LeCroix, R. F. Curl,
Peter M. McKinney and Rollie J. Myers

RECEIVED
LAWRENCE
RADIATION LABORATORY

APR 5 1974

LIBRARY AND
DOCUMENTS SECTION

March 1974

Prepared for the U. S. Atomic Energy Commission
under Contract W-7405-ENG-48

TWO-WEEK LOAN COPY

This is a Library Circulating Copy which may be borrowed for two weeks. For a personal retention copy, call Tech. Info. Division, Ext. 5545

LAWRENCE BERKELEY LABORATORY
UNIVERSITY OF CALIFORNIA
BERKELEY

LBL-2590
c.2

DISCLAIMER

This document was prepared as an account of work sponsored by the United States Government. While this document is believed to contain correct information, neither the United States Government nor any agency thereof, nor the Regents of the University of California, nor any of their employees, makes any warranty, express or implied, or assumes any legal responsibility for the accuracy, completeness, or usefulness of any information, apparatus, product, or process disclosed, or represents that its use would not infringe privately owned rights. Reference herein to any specific commercial product, process, or service by its trade name, trademark, manufacturer, or otherwise, does not necessarily constitute or imply its endorsement, recommendation, or favoring by the United States Government or any agency thereof, or the Regents of the University of California. The views and opinions of authors expressed herein do not necessarily state or reflect those of the United States Government or any agency thereof or the Regents of the University of California.

MICROWAVE SPECTRUM OF SILYL METHYL ETHER*

by

Charles D. LeCroix[+] and R. F. Curl

Chemistry Department, Rice University

Houston, Texas

and

Peter M. McKinney[‡] and Rollie J. Myers

Inorganic Materials Research Division of the Lawrence Berkeley Laboratory

and the Department of Chemistry, University of California

Berkeley, California

* This work was supported by National Science Foundation Grant GP-29374X and Grant C-071 of the Robert A. Welch Foundation.

+ Present Address: Wright-Patterson Air Force Base, Dayton, Ohio

‡ Present Address: University of Botswanana, Lesotho, Swaziland

Abstract

The microwave spectra of silyl methyl ether, SiH_3OCH_3, and its isotopic modifications, SiH_3OCD_3, SiD_3OCH_3, and SiD_3OCD_3, have been observed and assigned. Large splittings arising from the internal rotation of the methyl top and somewhat smaller splittings arising from the internal rotation of the silyl top are observed. The "effective barrier" to internal rotation of the methyl top is approximately 550 cal/mole. The "effective barrier" to internal rotation of the silyl top is approximately 1100 cal/mole. The internal rotation of the two tops is strongly coupled, but no values for the potential coupling constants have been obtained.

The dipole moment has been determined to be 1.15 ± 0.02 debye ($|\mu_a|$ = 0.647 ± 0.01 and $|\mu_b|$ = 0.95 ± 0.02 debye) from measurements of the Stark effect.

INTRODUCTION

The investigation of the microwave spectrum of silyl methyl ether (SiH_3OCH_3) was undertaken with the aims of determining the barriers to internal rotation, the molecular structure, and the dipole moment.

Very few double rotor, or "two top", molecules have been studied by microwave spectroscopy. Only recently was a detailed analysis of the internal rotation structure of two nonequivalent tops completed (1). The molecule studied was N-methyl-ethylidenimine, $CH_3CH{=}NCH_3$. It was found for this molecule that the two tops can be treated independently and the spectrum can be predicted within experimental accuracy.

Silyl methyl ether also has two nonequivalent tops which can undergo internal rotation. From the data and internal rotation analysis to be discussed below, it will become apparent that it is not possible to treat the two tops independently but rather some coupling between the tops must be introduced. Therefore, this is the first investigation where top-top coupling effects are readily apparent in the microwave spectrum and although somewhat unexpected, present a very interesting problem.

This investigation is the first to determine the barrier to internal rotation of a silyl group (SiH_3) attached to an oxygen atom. From Table I, it is seen that the barrier of a methyl group (CH_3) attached to an oxygen atom varies greatly among the previous molecules reported. (2,3,4,5,6) Thus, the determination of these two barriers in silyl methyl ether is of interest both as a test of present theoretical methods of predicting barriers and as an extension of present knowledge of such barriers.

The structures of silicon-containing compounds are of interest because of their anomalous behavior when compared to similar Group IVA

molecules. This can be illustrated by considering a few examples. The molecule methyl isocyanate (CH_3NCO) has a C-N-C bond angle of about 140° (7). The silicon analogue, SiH_3NCO, has a Si-N-C angle of 180° (8). However, the germyl analogue, GeH_3NCO, has a Ge-N-C bond angle of less than 180° (9). Also, trimethylamine, $(CH_3)_3N$, is nonplanar (10) while trisilyamine, $(SiH_3)_3N$, is planar (11). Similarly, dimethyl ether, $(CH_3)_2O$, has a bond angle of 111.7° (3), while in $(SiH_3)_2O$, disiloxane, the Si-O-Si bond angle has been investigated several times with bond angles varying from 140-155° in infrared studies (12) and a value of 144.1 ± 0.9° from an electron diffraction study (13).

Although a value for the Si-O-C bond angle in silyl methyl ether has been found by a recent electron diffraction investigation (14) to be 120.6 ± 0.9°, an independent determination of the angle by microwave spectroscopy is valuable because of the anomalous behavior of the silicon compounds which prevent reliable predictions from similar molecules.

The work reported here was started in Berkeley. After making an initial Q branch assignment, experimental work was terminated in Berkeley and the majority of the measurements reported were completed at Rice University.

EXPERIMENTAL

The samples of silyl methyl ether were prepared at Berkeley by reacting SiH_3I with CH_3OH following the method of Sternbach and MacDiarmid (15). The yield was about 10% and the reaction required 5 hours at -80°C. In the work at Rice, silyl methyl ether was prepared using the following reaction scheme suggest by Dr. Alan Robiette:

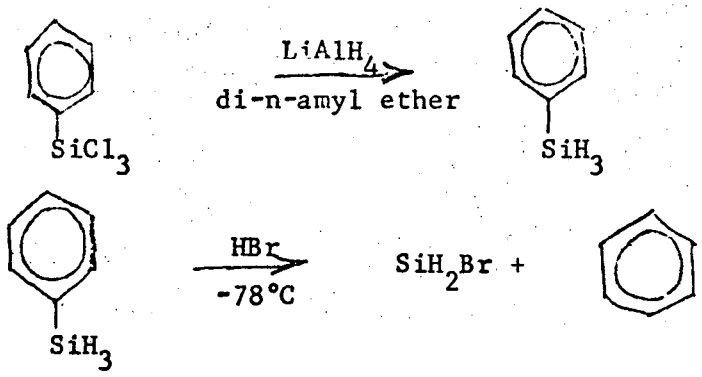

$$SiH_3Br \xrightarrow{HgCl_2} SiH_3Cl$$

$$3SiH_3Cl + 4NH_3 \xrightarrow[\text{phase}]{\text{gas}} (SiH_3)_3N + 3NH_4Cl$$

$$(SiH_3)_3N + 4HI \rightarrow 3SiH_3I + NH_4I$$

$$2SiH_3I \xrightarrow{HgS} (SiH_3)_2S$$

$$(SiH_3)_2S + 2CH_3OH \rightarrow 2SiH_3OCH_3 + H_2S$$

The deuterated species, SiH_3OCD_3, SiD_3OCH_3, and SiD_3OCD_3 were also prepared. The compound SiH_3OCD_3 was prepared using 99.5% CD_3OD (Bio-Rad Labs) in the last step of the reaction scheme. The silyl deuterated specie was prepared using $LiAlD_4$ (Stohler Isotope) in the first step of the reaction scheme. The fully deuterated specie was prepared using both $LiAlD_4$ and CD_3OD in the reaction scheme.

Although a long procedure, the yields obtained proved this a good method of preparing silyl methyl ether. The yields of the first two steps were less than 50%, but the remaining steps gave yields of 90-100%. Except for the first step, all work was done in a vacuum system.

The microwave spectrum of silyl methyl ether was first observed using klystron sources and Stark modulation. On the Berkeley instrument the klystrons were phase-locked to the harmonics of a frequency standard combined with a stable low frequency sweep oscillator. The modulation frequency was 5 kHz. The instrument at Rice was a conventional 100 kHz Stark-modulated spectrometer with oscilloscope display and phase sensitive detection with frequency measurement accuracy with ± 0.3 MHz. The frequency range was 8-40 GHz and the cell was always cooled to -78°C. Much of the work was done using a Hewlett-Packard 8460A MRR Spectrometer with chart recorder output of the spectrum. The frequency range on the Hewlett-Packard spectrometer was 26.5-40 GHz, and frequency measurements are within ± 0.05 MHz. The cell of the 8460A MRR spectrometer was kept at room temperature. All reported transition frequencies above 26.5 GHz were measured or checked on the Hewlett-Packard spectrometer.

Since silyl methyl ether is quantitatively hydrolyzed to disiloxane, $(SiH_3)_2O$, the waveguide was pumped down for several hours prior to sample introduction. Usually enough H_2O remained in the cell to react with the ether, thus causing the absorption lines to quickly disappear. After two or three sample introductions and pumpdowns, the ether remained in the cell and only slowly disappeared.

THEORY

Classical Kinetic Energy

The model used here to obtain the Hamiltonian for a two top system such as silyl methyl ether approximates the molecule as a rigid frame with two rigid rotating subgroups attached to the frame. The subgroups are assumed symmetrical about the axes on which they are constrained to rotate. This axis is fixed with respect to the main frame of the molecule. For such a system, the kinetic energy has been derived by Kilpatrick and Pitzer. (16) From their derivation, the following classical kinetic energy expression can be obtained:

$$2T = \frac{P_a^{\,2}}{I_a} + \frac{P_b^{\,2}}{I_b} + \frac{P_c^{\,2}}{I_c} + F_1\,(p_1 - \mathcal{P}_1)^2 + F_2\,(p_2 - \mathcal{P}_2)^2 + 2F_{12}\,(p_1 - \mathcal{P}_1)(p_2 - \mathcal{P}_2) \qquad (1)$$

where

P_i = component of total angular momentum along principal axis $\underline{i}$

I_i (a,b,c) = moment of inertia of the molecule about the $\underline{i}$th principal axis

$$F_1 = L_2/(L_2L_1 - \Lambda_{12}^2)$$

$$F_2 = L_1/(L_1L_2 - \Lambda_{12}^2)$$

$$F_{12} = \Lambda_{12}/(L_1L_2 - \Lambda_{12}^2)$$

$$L_j = I_j\left[1 - I_j \sum_{i=a,b,c} \frac{(\lambda_j^i)^2}{I_i}\right] \quad (j=1,2)$$

I_j (j=1,2) = moment of inertia of internal rotor $\underline{j}$ about its axis of internal rotation

λ_j^i (i=a,b,c)(j=1,2) = cosine of the angle between internal rotor j and principal axis i

$$\Lambda_{12} = \sum_{i=a,b,c} \frac{I_1 I_2 \lambda_1^i \lambda_2^i}{I_i}$$

p_j (j=1,2) = angular momentum of internal rotor j about its axis of internal rotation

$$\mathcal{P}_j = \sum_{i=a,b,c} P_i \frac{\lambda_j^i I_j}{I_i} \quad (j=1,2).$$

Potential Energy

The potential energy function in a molecule with one internal rotor is usually parameterized by an expansion in a Fourier series. For a rotor with a threefold axis of symmetry, the equation usually used for the potential function is given by

$$V(\varphi) = \frac{V_3}{2}(1 - \cos 3\varphi) + \frac{V_6}{2}(1 - \cos 6\varphi) + \ldots \qquad (2)$$

where the internal rotation angle is φ.

For two nonequivalent top molecules such as silyl methyl ether, the potential energy function is more complicated. For such molecules, the potential function contains terms for each top similar to those in a one top molecule, i.e., the tops are behaving independently. In addition, there are terms representating the possible potential interactions between the two tops. In such cases, therefore, the potential function can be described by two angles of internal rotation, φ_1 and φ_2. Ignoring sixfold terms, the parameters are two barrier heights, V_{31} and V_{32}, and two

interaction barrier terms, V_{12}^{c} and V_{12}^{s}. The total potential function can be written as

$$V(\varphi_1, \varphi_2) = \frac{V_{31}}{2}(1 - \cos 3\varphi_1) + \frac{V_{32}}{2}(1 - \cos 3\varphi_2) + V_{12}^{c}(1 - \cos 3\varphi_1)(1 - \cos 3\varphi_2) + V_{12}^{s} \sin 3\varphi_1 \sin 3\varphi_2 \tag{3}$$

For molecules published to date, it has not been necessary to include interactions between the two tops in order to fit the spectrum so that V_{12}^{c} and V_{12}^{s} have been assumed to be zero.

Total Quantum Mechanical Hamiltonian

The classical kinetic energy, (1), can be converted to the quantum mechanical equivalent with one modification: the term

$$2F_{12}(p_1 - \mathcal{P}_1)(p_2 - \mathcal{P}_2)$$

must be converted to

$$F_{12}[(p_1 - \mathcal{P}_1)(p_2 - \mathcal{P}_2) + (p_2 - \mathcal{P}_2)(p_1 - \mathcal{P}_1)]$$

when changing from classical to quantum mechanical notation because of the non-commutability of the operators contained in the $\mathcal{P}_i$'s.

Including the potential function just discussed, the total quantum mechanical Hamiltonian can be written after arranging terms:

$$H = H_{RR} \quad \frac{P_a^2}{I_a} + \frac{P_b^2}{I_b} + \frac{P_c^2}{I_c} +$$

$$H_{IR} \quad F_1 p_1^2 + \frac{V_{31}}{2}(1 - \cos 3\varphi_1) + F_2 p_2^2 + \frac{V_{32}}{2}(1 - \cos 3\varphi_2) +$$

$$H_{TT} \quad F_{12}(p_1p_2 + p_2p_1) + V^c_{12}\,(1 - \cos 3\varphi_1)(1 - \cos 3\varphi_2) + V^s_{12} \sin 3\varphi_1 \sin 3\varphi_2$$

$$H_{INT} \quad -2F_1p_1\mathcal{P}_1 - 2F_2p_2\mathcal{P}_2 - 2F_{12}(p_1\mathcal{P}_2 + p_2\mathcal{P}_1)$$

$$H_{ROT} \quad F_1\mathcal{P}_1^2 + F_2\mathcal{P}_2^2 + F_{12}\,(\mathcal{P}_1\mathcal{P}_2 + \mathcal{P}_2\mathcal{P}_1) \tag{4}$$

where

H_{RR} = rigid rotor Hamiltonian

H_{IR} = internal rotation of two independent tops

H_{TT} = top-top coupling

H_{INT} = interaction terms between tops and frame

H_{ROT} = overall rotation terms

In the limit of very high barriers, the effects of H_{INT} just cancel the effects of H_{ROT} and the molecule behaves as a rigid rotor.

Symmetry Considerations

The molecule silyl methyl ether can have a plane of symmetry if the silyl and methyl groups each have a hydrogen atom in the heavy atom plane. This was assumed to be the case (Fig. 1). The symmetry properties and group theoretical considerations of two nonequivalent top molecules have been previously reported by Dreizler (17).

Here the group theoretical treatment will be given in Molecular Symmetry Group language introduced by Longuet-Higgins (18). Silyl methyl

ether belongs to a molecular symmetry group whose character table is shown in Table II. This group, called Group 18, contains two non-degenerate irreducible representations and four doubly-degenerate irreducible representations. Therefore, the eigenvalues of the Hamiltonian are non-degenerate with symmetry A_1 or A_2 or doubly-degenerate with symmetry E_1, E_2, E_3, or E_4. Group 18 is a subgroup of the $C_{3V}^{-} \times C_{3V}^{+}$ group to which belong the more symmetric two top molecules such as acetone and dimethyl ether and whose group symmetry properties have been reported by Myers and Wilson (19).

Species of the Rotational and Torsional States, Selection Rules and Statistical Weights

By the standard procedures the species of the rotational and torsional wave functions were calculated and are listed in Table III.

The selection rules may be determined by finding the symmetry specie to which the dipole moment of the molecule belongs. From Fig. 1, the dipole moment components are seen to lie along the z and x axes, both of which belong to the A_2 species. This, in correlation with the multiplication table of the irreducible representations shown in Table IV, gives the selection rules and corresponding internal rotation components also shown in Table IV.

The relative intensities of these internal rotation species are given by the statistical weights. The operations of Group 18 which correspond to a permutation of the nuclei are to be considered. These operations are all of the operations of Group 18 except those belonging to the last class, and form an invariant subgroup of Group 18 of order 9 isomorphous with $C_{31} \otimes C_{32}$. The total wave function must be of symmetry A when reduced on this group. The total wave function is the direct

product of the nuclear spin wave function with the vibrational-torsional-rotational wave function. The character of the group $C_{31} \otimes C_{32}$ is given in Table V.

The characters of the nuclear spin functions are then reduced on the irreducible representations of $C_{31} \otimes C_{32}$ and the statistical weight of this irreducible representation, or internal rotation specie, is the number of times it appears in the reduction.

The statistical weights and relative intensities for the four molecular species of silyl methyl ether are shown in Table VI. Depending on the barrier heights of the silyl and methyl tops, five lines or less may be seen for each transition. If less, the relative intensity of certain lines will be the sum of the relative intensities of the component lines.

It is convenient to label the observed rotational transitions by the symbols AA, AE, EA, EE_+, or EE_- rather than by the molecular symmetry group labels A_1, A_2, E_1, E_2, E_3, and E_4, because the transitions AA always involve $A_1 \longleftrightarrow A_2$, and the AE, EA labels serve as a reminder about the torsional substate of each rotor. The label EE_+ means that $\sigma_1 = \sigma_2$ while the label EE_- means $\sigma_2 = -\sigma_1$.

SPECTRUM ASSIGNMENT

The microwave spectra of four species of silyl methyl ether (SiH_3OCH_3; SiH_3OCD_3; SiD_3OCH_3; SiD_3OCD_3) have been assigned. Only the procedure that was used to assign the normal specie, SiH_3OCH_3, will be given. Except for minor changes, the same procedure was used for all molecular species.

The normal molecular specie (SiH_3OCH_3) was first to be prepared and investigated. An initial prediction of the spectrum was made with the assumed structural values found in Table VII.

Using these predictions, a series of doublets with a spacing of about 28 MHz and the proper Stark effects to belong to the $J_{0J} \rightarrow J_{1,J-1}$ b-type Q branch series were found about 500 MHz above the predicted frequencies. Then the predictions were modified by varying the Si-O-C angle until the predicted lines fell reasonably close to the observed lines.

These predictions were used to search for the a-type R branch lines. The $0_{00} \rightarrow 1_{01}$, $1_{11} \rightarrow 2_{12}$, $1_{01} \rightarrow 2_{02}$, and $1_{10} \rightarrow 2_{11}$ lines were quickly identified. The $0_{00} \rightarrow 1_{01}$ line was found to be a doublet with a splitting of 9.23 MHz. If this splitting was interpreted as due to internal rotation of one top and used to estimate the internal rotation splitting of the b-type Q branches, the predicted splittings were several hundred MHz. The 28 MHz splitting observed for the b-type Q branches must then arise from internal rotation of the other top. It will become evident that the large splittings are associated with internal rotation of the methyl group and the smaller splittings are associated with internal rotation of the silyl group.

The search for the E species lines of the methyl top of the b-type Q branch series was most tedious on the conventional spectrometer. These were easily found as a three-line pattern on a scan taken with the Hewlett-Packard spectrometer. The doublet pattern already seen was extended to J = 10 and the E specie lines were observed to be triplets and could be seen also up to J = 10. The triplet pattern included one line as intense as the doublet and two lines half as intense. The five lines of each Q branch transition were assigned to the internal rotation states. The $10_{0,10} \rightarrow 10_{19}$ transition is depicted in Figure 2 with the internal rotation assignment.

Checks of the assignment of the normal molecular specie were made using cross-checks of the a- and b-type lines of the different series. Figure 3 indicates the method by which this cross-checking was made. For all five internal rotation species, the formulas in Figure 3 are applicable. Using these formulas, ν_8, ν_9, and ν_{10}, frequencies were calculated and compared to the observed frequencies. This was not only used as a check of the assignment, but was also used in locating certain species, i.e., the EA, EE_+ and EE_- species of the $1_{10} \rightarrow 2_{11}$, $2_{11} \rightarrow 3_{12}$, etc. The checks are shown in Table VII for all isotopic species.

The spectrum of the AA specie can be fitted using the rigid rotor model. Except for the lowest J members, the AE specie also fits the rigid rotor model. The lowest J members of the AE specie begin to move relative to the AA specie members because of the silyl internal rotation, and thus do not follow the rigid rotor model very well. The rotational constants obtained from such fits on the rigid rotor model of the AA and AE species are, of course, not the rotational constants of the molecule

because of the large effect that the internal rotations of both tops have on the spectrum. Because of the effects of internal rotation, the EA, EE_+, and EE_- species do not follow the rigid rotor model. In order to obtain the molecular rotational constants, a program accounting for all internal rotation effects must be used.

For SiH_3OCH_3, Figure 4 shows the patterns and relative movements of the species in the b-type Q branch series. The most interesting feature is that of the relative movements of the EE_+ and EE_- species. Table IX lists the frequencies of the species for assigned b-type lines. Figure 5 illustrates the patterns for the a-type R branch series, and Table X lists the frequencies of the species for assigned a-type lines.

The deuterated molecules (SiH_3OCD_3, SiD_3OCH_3, and SiD_3OCD_3) were assigned using the same approach as that described above for the normal molecular specie. Table VIII shows the cross-checks made for the a- and b-type lines of SiH_3OCD_3 using Figure 3. Tables XI and XII list the frequencies of the SiH_3OCD_3 species for assigned b- and a-type lines respectively. Table VIII provides the assignment checks for SiD_3OCH_3 while Tables XIII and XIV list the frequencies of the species of the assigned b- and a-type lines respectively. The molecule SiD_3OCD_3, whose internal rotation splittings are drastically reduced from those in the normal specie, was assigned and the assignment checks are listed in Table VIII. Tables XV and XVI list the frequencies of the assigned b- and a-type lines respectively.

The internal rotation pattern and relative intensities are compared for all species for the $10_{0,10} \rightarrow 10_{1,9}$ transition in Figure 6. It is

clear that the relative intensities indicate a pattern of statistical weights which clearly demonstrates that the larger internal rotation splittings are associated with the methyl top while the smaller splittings are associated with the silyl top.

DIPOLE MOMENT

The electric dipole moment of silyl methyl ether was determined by measuring the Stark lobes of the transitions shown in Table XVII. Second-order Stark measurements were made on three Stark lobes of two ground-state transitions of the normal specie with sample pressures of 20-30 mTorr, and with electric field value in the range 100-1000 V cm^{-1}.

The Stark cell was calibrated with OCS whose dipole moment has been determined to be μ_{OCS} = 0.71521 (0.00020) debye (20). The quantities μ_a and μ_b were obtained by a least squares fitting using the three determined Stark coefficients. The value of the total dipole moment $|\mu|$ = 1.15 ± .02 debye agrees well with the value of 1.166 debye obtained in an earlier polarization study (21).

INTERNAL ROTATION

According to equations (1) and (3) the effective Hamiltonian for the molecule is a function of eleven parameters, I_a, I_b, C, λ_1^a, λ_2^a, I_1, I_2, V_{31}, V_{32}, V_{12}^c, V_{12}^s. The internal rotation splittings of the observed frequencies are sensitive functions of λ_1^a, λ_2^a, I_1, I_2, and the four barrier parameters, but not the other three parameters. Since we can make reasonably accurate estimates of λ_1^a, λ_2^a, I_1, and I_2, the observed internal rotation splittings can be used to determine the barrier parameters. The estimates of the non-barrier parameters used are listed in Table XVIII.These estimates were obtained from the structure given in Table VII.

An estimate of the methyl barrier may be made from the observed splittings of the $0_{00} \rightarrow 1_{01}$ transition for the various isotopic species using the method of Kilb, Lin, and Wilson (22) and the tables of Herschbach (23) ignoring the presence of the silyl top. The estimates obtained from the observed splittings of the $0_{00} \rightarrow 1_{01}$ transition for the various isotopic species are shown in Table XIX. The b-type lines are affected strongly by the first order term $F_1W^{(1)}\alpha_1P_a$. The splitting of the EA from the AA line of the $1_{01} \rightarrow 1_{10}$ transition calculated from the observed splitting of the $0_{00} \rightarrow 1_{01}$ for SiH_3OCH_3 is compared with the observed splitting in Table XIX. The agreement while not excellent indicates that assignments are correct.

A barrier may be estimated for the silyl top by using the AA to AE splittings of low J b-type lines. The effect of the term $F_2W^{(1)}\alpha_2P_a$ while small is not negligible. For the SiH_3OCH_3 and SiD_3OCH_3 species the $0_{00} \rightarrow 1_{11}$ AA and AE species have been assigned. By averaging the

splittings of these lines with the splittings of the $1_{01} \rightarrow 1_{10}$ transitions the effects of the $F_2W^{(1)}\alpha_2P_a$ term may be cancelled. For the other species an estimate of the barrier may be made, and the second order perturbation effect of the term $F_2W^{(1)}\alpha_2P_a$ connecting the J_{1J} and $J_{1,J-1}$ levels calculated and added to the observed splitting. After the effect of $F_2W^{(1)}\alpha_2P_a$ is removed $\Delta\eta(=\Delta W^{(2)})$ may be calculated and s determined from the tables (23) by interpolation of $-\ln \Delta\eta$ versus $s^{\frac{1}{2}}$. The results of these calculations are shown in Table XX. The results obtained are reasonably self consistent and the direction and size of the barrier change on deuteration of the silyl group is typical (24).

It is not possible to extend this kind of analysis to the EE lines. The difficulty of such an extension can be easily understood by looking at the pattern of lines in the $2_{02} \rightarrow 2_{11}$ transition illustrated in Figure 4. The EA and EE calculations for the 2_{11} level are dominated by the $F_1W^{(1)}\alpha_1P_a$ term. The term $F_2W^{(1)}\alpha_2P_a$ adds to this term for the EE_- levels and subtracts from it for the EE_+ levels. Consequently, there is no way that the EE_- transition can be on the low frequency side of the EA transition if the two tops are assumed to be independent. Strong coupling between the torsions must be present.

The barriers calculated in Tables XIX and XX must, therefore, represent some sort of "effective barrier" and should not be interpreted as the V_{31} and V_{32} of equation (3).

A computer program for the CDC 6600 has been written to calculate the rotational frequencies for a molecule with two coupled inequivalent internal rotors. Because the barrier to internal rotation is quite small for the methyl top, the internal axis system which suppresses the

coupling off-diagonal in K of the methyl top was used. The torsional problem for each value of K for each top was solved using 15 free rotor basis functions for each symmetry. The terms coupling the two tops were set up in the free rotor basis and transformed to torsional eigenvalue basis. After truncating to seven functions for each top, the coupled torsional problem was set up giving a 49 x 49 matrix for each value of K and each of the five symmetries. The eigenvectors were saved and used to transform the coupling terms off diagonal in K ($\Delta K = \pm 1, \pm 2$). Each off diagonal in K block was then truncated to 10 x 10. The ground torsional state Hamiltonian matrix of dimensions (2J + 1) x (2J + 1) was formed by Van Vleck perturbation treatment of the 10 lowest torsional states. Finally this matrix was diagonalized and its eigenvalues used to calculate the rotational frequencies.

Checking the program presents formidable difficulties. No two coupled top calculations have been published to our knowledge. The program gives the results computed for N-methyl ethylidinimine without coupling by Maier, Bauder, and Gunthard (1). A completely independent program which calculates the coupled torsional energy levels from a free rotor basis by diagonalizing a 99 x 99 matrix checks with this program. Finally, the same frequencies result (with different symmetry labels) when the two tops are interchanged if both barriers are reasonably high so that use of the IAM method for the lower barrier top is not essential.

The correctness of the computer program has not been checked by fitting the spectrum of silyl methyl ether, because we have been unable to find a set of barrier parameters which qualitatively reproduces the

internal rotation patterns of the EA and EE transitions of the b-type Q branches. These are four barrier parameters, V_{31}, V_{32}, V_{12}^{c}, and V_{12}^{s} (see equation 3). It is clear that the potential coupling is large (i.e., either $|V_{12}^{c}|$ or $|V_{12}^{s}| \gg 0$). Possibly the four dimensional search over the barrier parameters has not been extensive enough. This molecule presents an interesting opportunity for further work.

ACKNOWLEDGEMENTS

The Berkeley work was conducted under the auspices of the U.S. Atomic Energy Commission. We would also like to thank Professor W. D. Gwinn for the use of his mocrowave spectrograph, and Dr. Alan Robiette for very helpful suggestions on sample preparation.

REFERENCES

1. J. Meier, A. Bauder, and Hs. H. Gunthard, J. Chem. Phys. 57, 1219 (1972).

2. R. F. Curl, Jr., J. Chem. Phys. 30, 1529 (1959).

3. P. H. Kasai and R. J. Myers, J. Chem. Phys. 30, 1096 (1959).

4. E. V. Ivash and D. M. Dennison, J. Chem. Phys. 21, 1804 (1953).

5. J. S. Rigden and S. S. Butcher, J. Chem. Phys. 40, 2109 (1964).

6. W. B. Dixon and E. B. Wilson, Jr., J. Chem. Phys. 35, 191 (1961).

7. R. F. Curl, Jr., V. M. Rao, K. V. L. N. Sastry, and J. A. Hodgeson, J. Chem. Phys. 39, 3335 (1963).

8. E. A. V. Ebsworth, D. R. Jenkins, M. J. Mays, and T. M. Sugden, J. Chem. Soc. 1963, 21 (1963).

9. K. R. Ramaprasad, R. Varmi, and R. Nelson, J. Am. Chem. Soc. 90, 6247 (1968).

10. D. R. Lide, Jr. and D. R. Mann, J. Chem. Phys. 28, 572 (1958).

11. K. Hedberg, J. Am. Chem. Soc. 77, 6491 (1955).

12. R. F. Curl, Jr., and K. S. Pitzer, J. Am. Chem. Soc. 80, 2371 (1958).

    D. W. Robinson, W. J. Lafferty, J. R. Aronson, J. R. Durig, and R. C. Lord, J. Chem. Phys. 35, 2245 (1961).

13. A. Almenningen, O. Bastiansen, V. Ewing, K. Hedberg, and M. Traetteberg, Acta Chem. Scand. 17, 2455 (1963).

14. C. Glidewell, D. W. H. Rankin, A. G. Robiette, G. M. Sheldrick, B. Beagley, and J. M. Freeman, J. Mol. Struct. 5, 417 (1970).

15. B. Sternbach and A. G. MacDiarmid, J. Am. Chem. Soc., 83, 3385 (1961).

16. J. E. Kilpatrick and K. S. Pitzer, J. Chem. Phys., 17, 1064 (1949).

17. H. Dreizler, Z. Naturforsh., 16A, 477 (1961).

18. H. C. Longuet-Higgins, Molecular Physics, 6, 445 (1963).

19. R. J. Myers and E. B. Wilson, Jr., J. Chem. Phys., 33, 186 (1960).

20. J. S. Muenter, J. Chem. Phys., 48, 4544 (1968).

21. R. Varma, A. G. MacDiarmid, and J. G. Miller, Inorg. Chem., 3, 1754 (1964).

22. R. W. Kilb, C. C. Lin, and E. B. Wilson, J. Chem. Phys. 26, 1695 (1957).

23. D. R. Herschbach, J. Chem. Phys. 27, 975 (1957).

24. D. Coffey, C. O. Britt, and J. E. Boggs, J. Chem. Phys. 49, 591 (1968).

TABLE I

METHYL BARRIERS IN COMPOUNDS CH_3-OX

Molecule	V(cal/mole)	References
CH_3OCHO	1190	(2)
CH_3OCH_3	2720	(3)
CH_3OH	1070	(4)
CH_3OCl	3060	(5)
CH_3ONO_2	2321	(6)

TABLE II

GROUP 18 CHARACTER TABLE

	E	2(123)	2(456)	2(123)(456)	2(132)(456)	9(23)(56)*
A_1	1	1	1	1	1	1
A_2	1	1	1	1	1	-1
E_1	2	2	-1	-1	-1	0
E_2	2	-1	2	-1	-1	0
E_3	2	-1	-1	2	-1	0
E_4	2	-1	-1	-1	2	0

TABLE III

SYMMETRY SPECIES OF ROTATIONAL AND TORSIONAL STATES

Rotational States

K_{-1}	K_{+1}	
e	e	A_1
o	e	
e	o	A_2
o	o	

Torsional States

v_1 v_2	
(0,0)	A_1, E_1, E_2, E_3, E_4
(1,0)	A_2, E_1, E_2, E_3, E_4
(0,1)	A_2, E_1, E_2, E_3, E_4
(1,1)	A_1, E_1, E_2, E_3, E_4

TABLE IV

MULTIPLICATION TABLE OF GROUP 18 SPECIES

	A_1	A_2	E_1	E_2	E_3	E_4
A_1	A_1	A_2	E_1	E_2	E_3	E_4
A_2	A_2	A_1	E_1	E_2	E_3	E_4
E_1	E_1	E_1	$A_1+A_2+E_1$	E_3+E_4	E_2+E_4	E_2+E_3
E_2	E_2	E_2	E_3+E_4	$A_1+A_2+E_2$	E_1+E_4	E_1+E_3
E_3	E_3	E_3	E_2+E_4	E_1+E_4	$A_1+A_2+E_3$	E_1+E_2
E_4	E_4	E_4	E_2+E_3	E_1+E_3	E_1+E_2	$A_1+A_2+E_4$

Selection Rules	Internal Rotation Specie
$A_1 \longleftrightarrow A_2$	AA
$E_1 \longleftrightarrow E_1$	EA
$E_2 \longleftrightarrow E_2$	AE
$E_3 \longleftrightarrow E_3$	EE_-
$E_4 \longleftrightarrow E_4$	EE_+

TABLE V

CHARACTER TABLE OF $C_{31} \times C_{32}$

	E	(123)	(132)	(456)	(465)	(123)(456)	(132)(456)	(123)(465)	(132)(465)
A	1	1	1	1	1	1	1	1	1
E_1	1	1	1	ϵ	ϵ^*	ϵ	ϵ	ϵ^*	ϵ^*
	1	1	1	ϵ^*	ϵ	ϵ^*	ϵ^*	ϵ	ϵ
E_2	1	ϵ	ϵ^*	1	1	ϵ	ϵ^*	ϵ	ϵ^*
	1	ϵ^*	ϵ	1	1	ϵ^*	ϵ	ϵ^*	ϵ
E_3	1	ϵ^*	ϵ	ϵ	ϵ^*	1	ϵ^*	ϵ	1
	1	ϵ	ϵ^*	ϵ^*	ϵ	1	ϵ	ϵ^*	1
E_4	1	ϵ	ϵ^*	ϵ	ϵ^*	ϵ^*	1	1	ϵ
	1	ϵ^*	ϵ	ϵ^*	ϵ	ϵ	1	1	ϵ^*

$A \times A = A$

$E_1 \times E_1 = E_1 + 2A$

$E_2 \times E_2 = E_2 + 2A$

$E_3 \times E_3 = E_3 + 2A$

$E_4 \times E_4 = E_4 + 2A$

$\epsilon = e^{2\pi i/3}$

TABLE VI

STATISTICAL WEIGHTS

	Specie	Statistical Weight	Relative Intensity
SiH_3OCH_3	AA	8	2
	AE	8	2
	EA	8	2
	EE_+	4	1
	EE_-	4	1
SiH_3OCD_3	AA	44	11
	AE	44	11
	EA	64	16
	EE_+	32	8
	EE_-	32	8
SiD_3OCH_3	AA	44	11
	AE	64	16
	EA	44	11
	EE_+	32	8
	EE_-	32	8
SiD_3OCD_3	AA	121	121
	AE	176	176
	EA	176	176
	EE_+	176	128
	EE_-	128	128

TABLE VII

ASSUMED STRUCTURAL VALUES OF

SiH_3OCH_3

FOR SPECTRUM PREDICTION

r_{Si-O}	1.63 Å
r_{C-O}	1.427 Å
r_{Si-H}	1.48 Å
r_{C-H}	1.09 Å
⟨Si-O-C	121.2°
⟨H-C-H	109.5°
⟨H-Si-H	109.5°

TABLE VIII

ASSIGNMENT CHECKS‡

Molecule	Transition	AA	AE	EA	EE_+	EE_-
SiH_3OCH_3	ν_8: $1_{10} \rightarrow 2_{11}$	22376.98 (0.08)	22375.56 (0.21)	22052.13 (-0.46)	a	a
	ν_9: $2_{11} \rightarrow 3_{12}$	33562.63 (-0.18)	33562.04 (-0.05)	33185.33 (0.31)	33187.68 (-0.10)	33185.33 (0.22)
SiH_3OCD_3	ν_8: $1_{10} \rightarrow 2_{11}$	19533.98 (-0.26)	19533.98 (0.21)	a	a	a
	ν_9: $2_{11} \rightarrow 3_{12}$	29298.84 (0.08)	29298.84 (b)	29250.87 (0.63)	29253.18 (-0.89)	29250.87 (0.37)
	ν_{10}: $3_{12} \rightarrow 4_{13}$	39061.39 (0.08)	39061.39 (b)	39033.10 (0.17)	39034.45 (0.17)	39033.10 (0.31)
SiD_3OCH_3	ν_8: $1_{10} \rightarrow 2_{11}$	20245.91 (-0.10)	20245.91 (-0.36)	a	a	a
	ν_9: $2_{11} \rightarrow 3_{12}$	30365.98 (0.14)	39365.98 (0.15)	a	a	a
SiD_3OCD_3	ν_{10}: $3_{12} \rightarrow 4_{13}$	35529.79 (0.02)	35529.79 (0.03)	35518.41 (0.10)	35518.41 (0.10)	35518.41 (0.10)

‡ Frequencies listed are observed; numbers in parentheses are observed-calculated.

a Not measured.

b Unavailable because $3_{03} \rightarrow 3_{12}$ AE line was not measured because of experimental difficulties.

TABLE IX

ASSIGNED b-TYPE LINES FOR SiH_3OCH_3

Transition	AA	AE	EA	EE_+	EE_-
$1_{01} \rightarrow 1_{10}$	28482.05	28457.70	29678.86	a	a
$2_{02} \rightarrow 2_{11}$	28858.82	28832.91	29749.48	29719.24	29732.37
$3_{03} \rightarrow 3_{12}$	29430.85	29404.39	29970.85	29943.37	29953.83
$4_{04} \rightarrow 4_{13}$	30206.34	30179.61	30431.58	30408.51	30414.83
$4_{14} \rightarrow 5_{05}$	28461.33	28487.65	a	a	a
$0_{00} \rightarrow 1_{11}$	39110.53	39081.29	a	a	a
$5_{05} \rightarrow 5_{14}$	31195.98	31169.15	31178.10	31159.75	31161.69
$6_{06} \rightarrow 6_{15}$	32413.17	32386.23	32217.88	32203.56	32201.56
$7_{07} \rightarrow 7_{16}$	33873.38	33846.32	33546.75	33535.60	33530.51
$8_{08} \rightarrow 8_{17}$	35594.13	33567.06	35164.64	35155.66	35148.35
$9_{09} \rightarrow 9_{18}$	37594.38	37567.25	37077.82	37070.52	37061.51
$10_{0,10} \rightarrow 10_{19}$	39893.78	39866.68	39297.61	39291.48	39281.31

a Not measured.

TABLE X

ASSIGNED a-TYPE LINES FOR SiH_3OCH_3

Transition	AA	AE	EA	EE_+	EE_-
$0_{00} \rightarrow 1_{01}$	11002.17	11002.17	10992.94	10992.94	10992.94
$1_{01} \rightarrow 2_{02}$	22000.13	22000.13	21981.98	21981.97	21981.97
$1_{10} \rightarrow 2_{11}$	22376.98	22375.56	22052.13	a	a
$1_{11} \rightarrow 2_{12}$	21630.38	21631.84	21930.37	a	a
$2_{02} \rightarrow 3_{03}$	32990.51	32990.51	32963.59	32963.59	32963.59
$2_{11} \rightarrow 3_{12}$	33562.63	33562.04	33185.33	33187.68	33185.33
$2_{12} \rightarrow 3_{13}$	32442.60	a	32782.25	a	a

a Not measured.

TABLE XI

ASSIGNED b-TYPE LINES FOR SiH_3OCD_3

Transition	AA	AE	EA	EE+	EE-
$1_{01} \rightarrow 1_{10}$	22758.58	22750.50	a	a	a
$2_{02} \rightarrow 2_{11}$	23049.31	23040.78	22972.66	22968.50	22965.76
$3_{03} \rightarrow 3_{12}$	23490.30	a	23371.90	23367.48	23367.48
$4_{04} \rightarrow 4_{13}$	24087.82	24079.20	23948.37	23943.83	23945.30
$5_{05} \rightarrow 5_{14}$	24850.00	24841.32	24698.12	24693.29	24695.48
$6_{06} \rightarrow 6_{15}$	25786.51	25777.80	25624.81	25619.98	25623.08
$7_{07} \rightarrow 7_{16}$	26909.34	26900.55	26738.77	26734.01	26737.30
$8_{08} \rightarrow 8_{17}$	28231.30	28222.49	28052.51	28047.54	28051.20
$9_{09} \rightarrow 9_{18}$	29766.76	29757.84	29579.32	29574.27	29577.97
$10_{0,10} \rightarrow 10_{19}$	31530.59	31521.68	31333.69	31328.60	31332.39
$11_{0,11} \rightarrow 11_{1,10}$	33537.82	33528.85	33330.47	33325.31	33329.66
$12_{0,12} \rightarrow 12_{1,11}$	35802.90	35793.89	35583.91	35578.62	35582.51
$13_{0,13} \rightarrow 13_{1,12}$	38338.81	38329.80	38106.83	38101.42	38105.19
$4_{14} \rightarrow 5_{05}$	26852.36	26860.66	a	a	a
$5_{15} \rightarrow 6_{06}$	37110.88	37119.14	a	a	a

a Not measured.

TABLE XII

ASSIGNED a-TYPE LINES FOR SiH_3OCD_3

Transition	AA	AE	EA	EE_+	EE_-
$0_{00} \rightarrow 1_{01}$	9624.44	9624.44	9621.19	9621.19	9621.19
$1_{01} \rightarrow 2_{02}$	19243.51	19243.51	19239.50	19239.50	19239.50
$1_{10} \rightarrow 2_{11}$	19533.98	19533.98	a	a	a
$1_{11} \rightarrow 2_{12}$	18957.82	18957.82	a	a	a
$2_{02} \rightarrow 3_{03}$	28857.77	28857.77	28852.26	28852.26	28852.26
$2_{11} \rightarrow 3_{12}$	29298.84	29298.84	29250.87	29253.18	29250.87
$2_{12} \rightarrow 3_{13}$	28434.44	28434.44	28473.46	a	a
$3_{03} \rightarrow 4_{04}$	38463.79	38463.79	38456.46	38456.46	38456.46
$3_{12} \rightarrow 4_{13}$	39061.39	39061.39	39033.10	39034.45	39033.10
$3_{13} \rightarrow 4_{14}$	37908.89	37908.89	37925.24	37923.87	37925.24

a Not measured.

TABLE XIII

ASSIGNED b-TYPE LINES FOR SiD_3OCH_3

Transition	AA	AE	EA	EE_+	EE_-
$1_{01} \rightarrow 1_{10}$	19502.80	19498.40	a	a	a
$2_{02} \rightarrow 2_{11}$	19810.16	19806.02	20371.29	a	a
$3_{03} \rightarrow 3_{12}$	20277.48	20273.33	20603.13	a	a
$4_{04} \rightarrow 4_{13}$	20912.34	20908.08	21055.64	a	a
$5_{05} \rightarrow 5_{14}$	21727.41	21723.34	21741.78	a	a
$6_{06} \rightarrow 6_{15}$	22733.27	22728.79	22659.01	a	a
$7_{07} \rightarrow 7_{16}$	23942.74	23938.26	23805.56	23806.31	23803.78
$8_{08} \rightarrow 8_{17}$	25379.43	25375.18	25186.19	25186.89	25184.32
$9_{09} \rightarrow 9_{18}$	27053.72	27049.73	26811.44	26812.25	25809.52
$10_{0,10} \rightarrow 10_{19}$	28986.04	28982.00	28694.54	28695.48	28692.91
$11_{0,11} \rightarrow 11_{1,10}$	31192.98	31188.89	30849.73	30850.99	30848.26
$12_{0,12} \rightarrow 12_{1,11}$	33689.27	33685.24	33290.34	33291.38	33288.81
$13_{0,13} \rightarrow 13_{1,12}$	36486.81	36482.81	36026.94	36028.02	36025.45
$14_{0,14} \rightarrow 14_{1,13}$	39593.46	39589.47	39067.03	39068.03	39065.57
$0_{00} \rightarrow 1_{11}$	29170.22	29165.68	a	a	a
$4_{14} \rightarrow 5_{05}$	31906.52	a	a	a	a

a Not measured.

TABLE XIV

ASSIGNED a-TYPE LINES FOR SiD_3OCH_3

Transition	AA	AE	EA	EE_+	EE_-
$0_{00} \rightarrow 1_{01}$	9971.16	9971.16	9964.81	9964.81	9964.81
$1_{01} \rightarrow 2_{02}$	19938.65	19938.65	19926.15	19926.15	19926.15
$1_{10} \rightarrow 2_{11}$	20245.91	20245.91	a	a	a
$1_{11} \rightarrow 2_{12}$	19638.19	19638.19	a	a	a
$2_{02} \rightarrow 3_{03}$	29898.52	29898.52	29879.60	29879.60	29879.60
$2_{11} \rightarrow 3_{12}$	30365.98	30365.98	a	a	a
$2_{12} \rightarrow 3_{13}$	29454.67	29454.67	a	a	a
$3_{03} \rightarrow 4_{04}$	39847.59	39847.59	39823.15	39823.15	39823.15
$3_{13} \rightarrow 4_{14}$	39268.38	39268.38	a	a	a

a Not measured.

TABLE XV

ASSIGNED b-TYPE LINES FOR SiD_3OCD_3

Transition	AA	AE	EA	EE_+	EE_-
$3_{03} \rightarrow 3_{12}$	17218.65	17217.56	17172.46	17172.46	17172.46
$4_{04} \rightarrow 4_{13}$	17712.65	17711.55	17659.01	17659.01	17659.01
$5_{05} \rightarrow 5_{14}$	18344.11	18343.17	18283.79	18283.79	18283.79
$6_{06} \rightarrow 6_{15}$	19122.58	19121.42	19057.63	19057.63	19057.63
$7_{07} \rightarrow 7_{16}$	20058.29	20057.19	19989.29	19989.29	19989.29
$8_{08} \rightarrow 8_{17}$	21163.52	21162.34	21090.00	21090.00	21090.00
$9_{09} \rightarrow 9_{18}$	22450.77	22449.65	22371.80	22371.80	22371.80
$10_{0,10} \rightarrow 10_{19}$	23933.49	23932.13	23848.00	23848.00	23848.00
$11_{0,11} \rightarrow 11_{1,10}$	25624.40	25623.25	25532.13	25532.13	25532.13
$12_{0,12} \rightarrow 12_{1,11}$	27535.52	27534.52	27435.79	27436.18	27435.47
$13_{0,13} \rightarrow 13_{1,12}$	29677.11	29676.11	29568.91	29569.29	29568.59
$14_{0,14} \rightarrow 14_{1,13}$	32056.68	32055.68	31939.04	31939.41	31938.73
$15_{0,15} \rightarrow 15_{1,14}$	34678.45	34677.45	34550.52	34550.85	34550.18
$16_{0,16} \rightarrow 16_{1,15}$	37542.92	37541.92	37403.72	37404.02	37403.37

TABLE XVI

ASSIGNED a-TYPE LINES FOR SiD_3OCD_3

Transition	AA	AE	EA	EE_+	EE_-
$0_{00} \rightarrow 1_{01}$	8765.82	8765.82	8764.84	8764.84	8764.84
$1_{10} \rightarrow 2_{11}$	17767.71	17767.71	a	a	a
$1_{11} \rightarrow 2_{12}$	17294.09	17294.09	a	a	a
$2_{11} \rightarrow 3_{12}$	26649.92	26649.92	26632.06	26632.06	26632.06
$3_{03} \rightarrow 4_{04}$	35035.77	35035.77	35031.76	35031.76	35031.76
$3_{13} \rightarrow 4_{14}$	34582.13	34582.13	34586.40	34586.40	34586.40
$3_{12} \rightarrow 4_{13}$	35529.79	35529.79	35518.41	35518.41	35518.41

a Not measured.

TABLE XVII

STARK EFFECT AND DIPOLE MOMENT

Transition[a]	M	Stark Coefficients (MHz./[V^2/cm^2]) x 10^{+6}	
		Obs.	Calc.
$0_{00} \rightarrow 1_{01}$	0	6.171	6.172
$1_{01} \rightarrow 2_{02}$	0	-3.750	-3.748
$1_{01} \rightarrow 2_{02}$	1	0.752	0.747

$$\mu_a = 0.647 \pm 0.006$$

$$\mu_b = 0.95 \pm 0.02$$

$$|\mu| = 1.15 \pm 0.02$$

[a]All transitions of internal rotation species AA.

TABLE XVIII

NON-BARRIER PARAMETERS USED IN INTERNAL ROTATION CALCULATIONS

	CH_3OSiH_3	CD_3OSiH_3	CH_3OSiD_3	CD_3OSiD_3
I_a (u Å^2)	15.059	18.297	20.643	23.856
I_b (u Å^2)	88.513	101.329	98.091	111.676
C (MHz)	5353.28	4710.52	4872.56	4306.73
λ_1^a	0.8177	0.8309	-0.9169	0.8290
λ_2^a	-0.9158	-0.9063	-0.9169	-0.9077
I_1 (u Å^2)	3.22	6.44	3.22	6.44
I_2 (u Å^2)	5.94	5.94	11.87	11.87
F_1^a (MHz)	185520.	106370	177095	98479.
F_2^a (MHz)	129215.	117652	85438	73835.

[a] Calculated from one top formula. No coupling included.

TABLE XIX

ESTIMATES OF THE CH_3 BARRIER

	CH_3OSiH_3	CD_3OSiH_3	CH_3OSiD_3	CD_3OSiD_3
$0_{00} \rightarrow 1_{01}$				
$\Delta\nu$(MHz)	9.23	3.25	6.35	0.98[a]
S	14	22.4	14.5	27.8
V_1(cal/mole)	557	510	550	586

$1_{01} \rightarrow 1_{10}$	CH_3OSiH_3		
		Obs.	Calc.[b]
	$(\nu_{AA} - \nu_{EA})$(MHz)	-1196.81	-1272

[a] The observed splitting may be somewhat smaller than the true splitting because of overlap.

[b] From the observed splittings of the $0_{00} \rightarrow 1_{01}$ transition and $F_1(W^{(1)}\rho_1 + W^{(2)}\rho_1^2)$ using the parameters of Table XXI.

TABLE XX

ESTIMATES OF THE SILYL BARRIER

SiH_3OCH_3

	$\Delta\nu$ (AA - AE)	
	$0_{00} \rightarrow 1_{11}$	29.24
	$1_{01} \rightarrow 1_{10}$	24.35
	Ave.	26.79 MHz
	$\Delta\eta$	1.595×10^{-3}
	S	40
	V_2	1110 cal/mole

SiH_3OCD_3

$1_{01} \rightarrow 1_{10}$	$\Delta\nu$ (AA - AE)	8.08 MHz
	$\frac{(F_2W^{(1)}\alpha_2P_a)^2}{B - C}$	1.55
	$F_2\ \alpha_2^2\ \Delta\eta$	9.63 MHz
	$\Delta\eta$	9.45×10^{-4}
	S	43.8
	V_2	1108 cal/mole

TABLE XX (Continued)

SiD_3OCH_3

$\Delta\nu$ (AA - AE)	
$0_{00} \rightarrow 1_{11}$	4.54 MHz
$1_{01} \rightarrow 1_{10}$	4.40
Ave.	4.47 MHz
$\Delta\eta$	1.89×10^{-4}
S	57.0
V_2	1045 cal/mole

SiD_3OCD_3

$\Delta\nu$ (AA - AE)	
$3_{03} \rightarrow 3_{12}$	1.09 MHz
$W^{(1)}$ corr.	--
	1.09
$\Delta\eta$	7.23×10^{-5}
S	67
V_2	1060 cal/mole

Legends for Figures

Figure 1. Assumed structure of silyl methyl ether showing the labelling of the hydrogen atoms. Note that the molecule is assumed to have C_s symmetry with H_5 below the plane and H_2 above the plane. The internal rotation angle, φ_1, increases by $2\pi/3$ as the result of the operation (1,2,3). The internal rotation angle φ_2 increases by $2\pi/3$ as a result of the operation (4,5,6).

Figure 2. Observed internal rotation splitting pattern for the $10_{0,10} \rightarrow 10_{1,9}$ transition of SiH_3OCH_3 showing the intensities determined by statistical weights. Note that the EA, EE_+, and EE_- Stark effect is much more rapid than that of AA and AE. The marker spacings are 1 MHz.

Figure 3. An illustration of the energy level scheme which leads to the frequency sum rules which provide cross checks of the assignment.

Figure 4. The J dependence of the internal rotation structure of the b-type Q branches $J_{0J} \rightarrow J_{1,J-1}$ of SiH_3OCH_3. For low J the AA to EA spacing is largely determined by the term $F_1W^{(1)}\alpha_1P_a$ connecting $J_{1,J}$ to $J_{1,J-1}$ which shifts the EA line up. For high J this term becomes less important because the rigid rotor energy difference $J_{1,J}$ to $J_{1,J-1}$ is approximately $(\frac{B-C}{2})J(J+1)$.

Figure 5. The a-type R branch patterns for K = 0 and 1 observed for SiH_3OCH_3. The silyl internal rotation splittings are not resolved. The K = 1 lines of symmetry E(EA, EE_+, EE_-)

cluster near the center in the characteristic manner normally observed for one top molecules with a low barrier to internal rotation.

Figure 6. Internal rotation pattern, relative intensities, and statistical weights of the $10_{0,10} \rightarrow 10_{1,9}$ transition for the four isotopic species of silyl methyl ether studied.

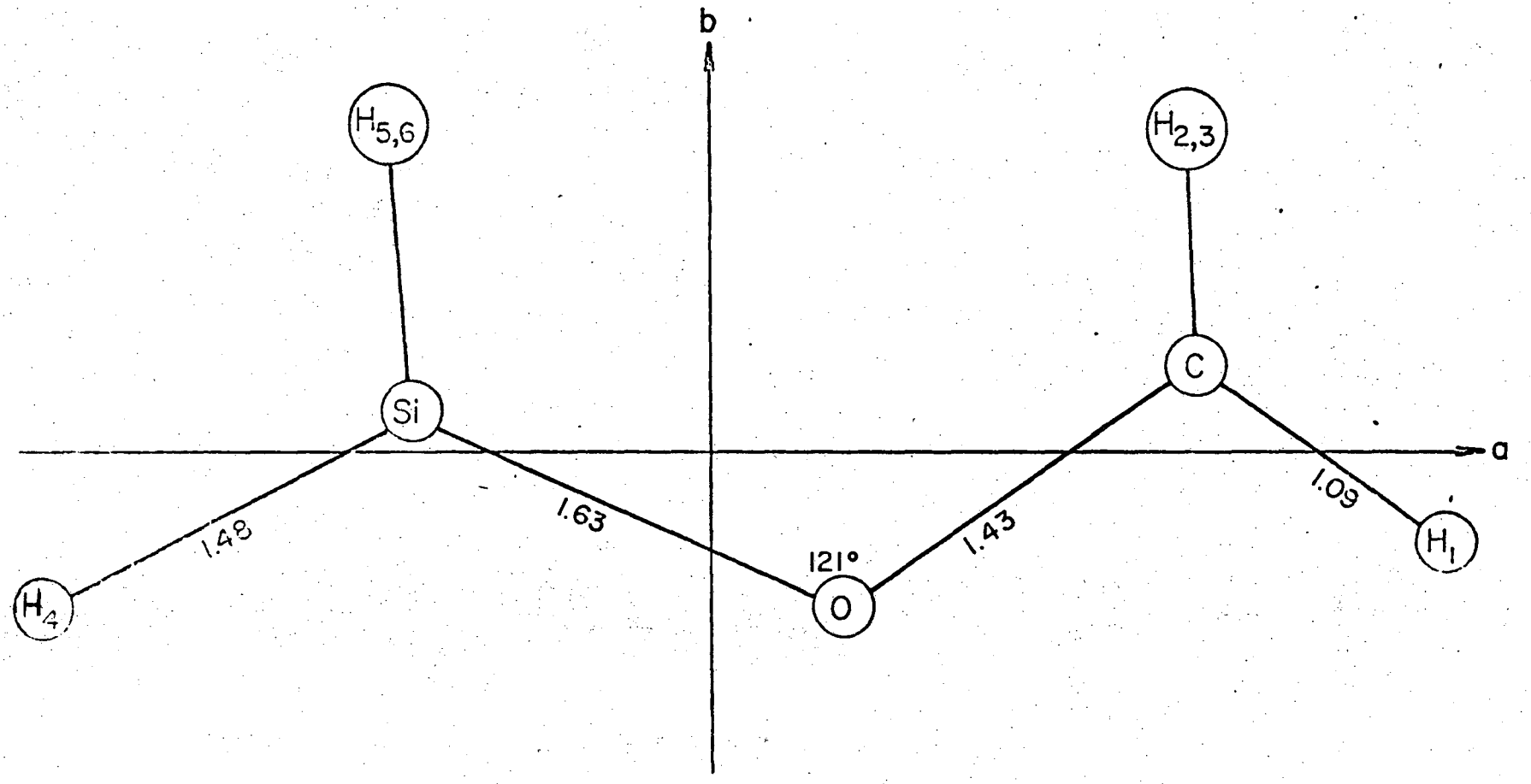

Fig. 1

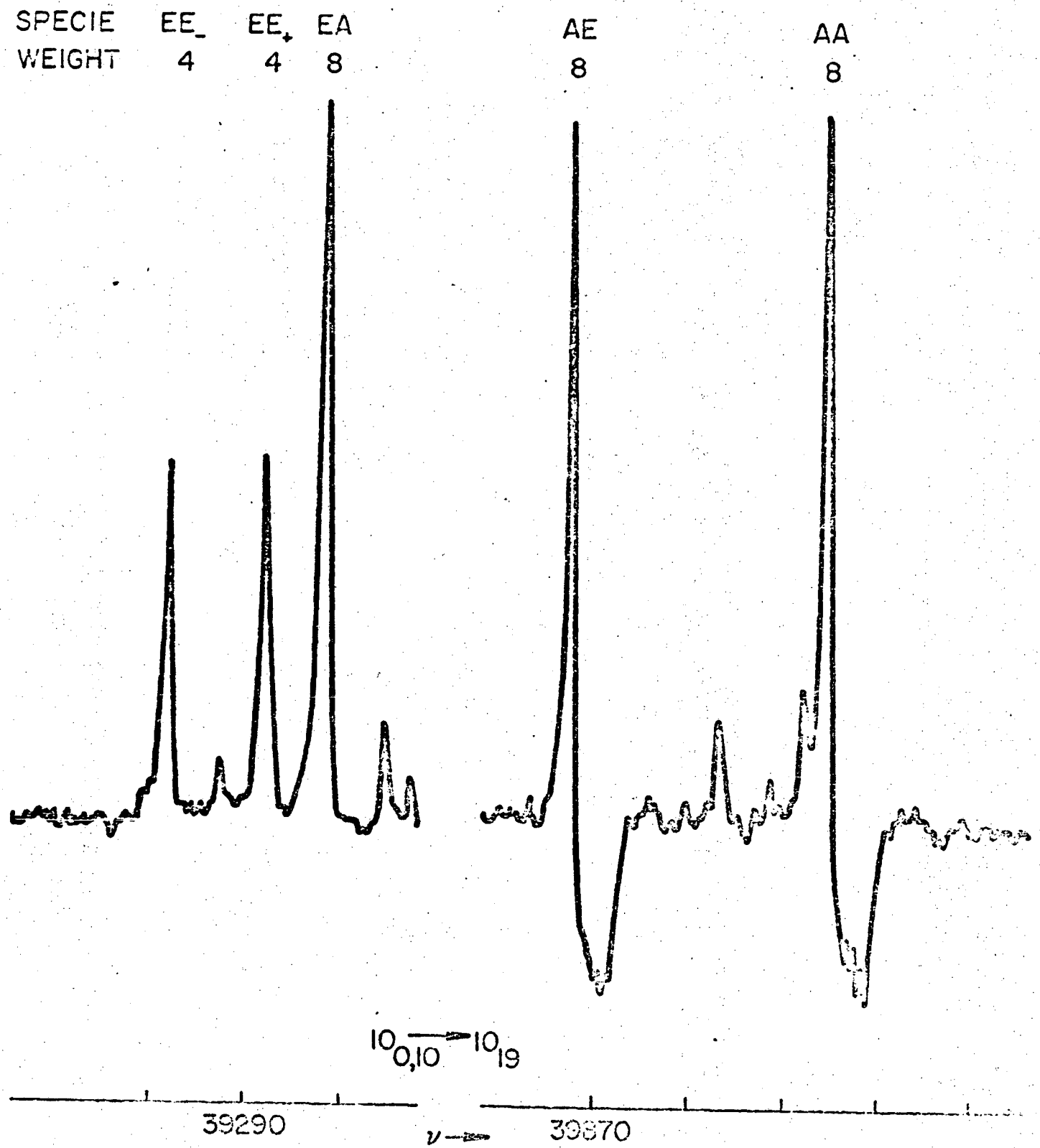
SPECIE
WEIGHT
EE_
4
EE+
4
EA
8
AE
8
AA
8
$10_{0,10} \rightarrow 10_{19}$
39290
ν
39870

Fig. 2

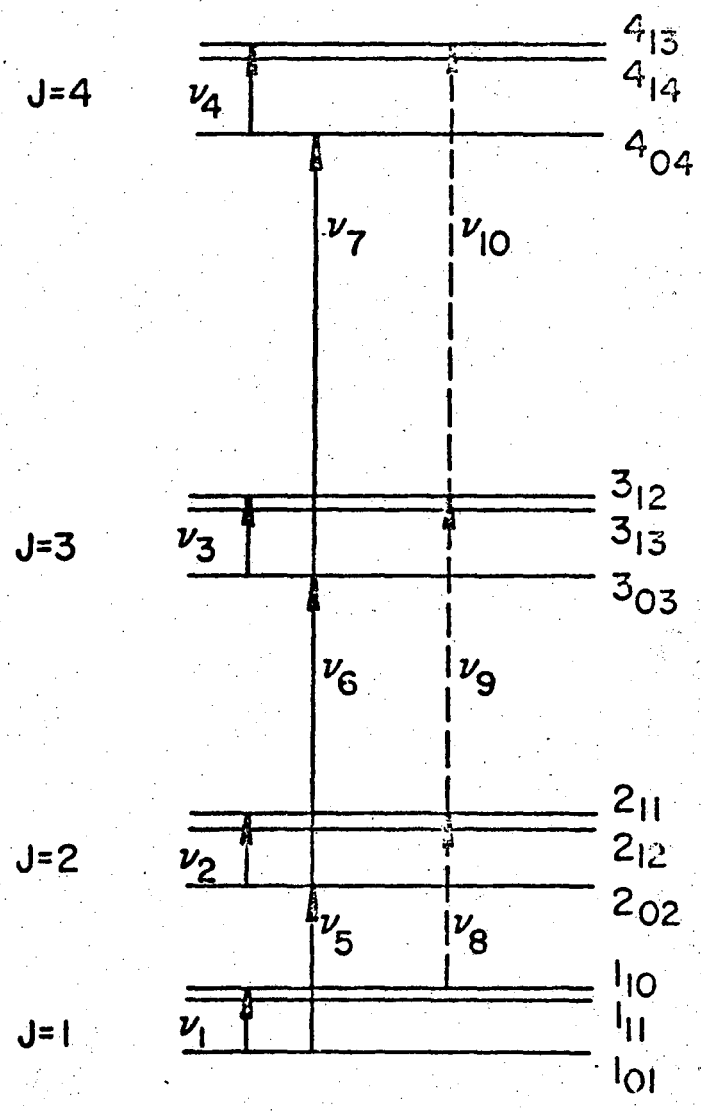

$$\nu_8 = \nu_5 + \nu_2 - \nu_1$$

$$\nu_9 = \nu_6 + \nu_3 - \nu_2$$

$$\nu_{10} = \nu_7 + \nu_4 - \nu_3$$

Fig. 3

SiH_3OCH_3

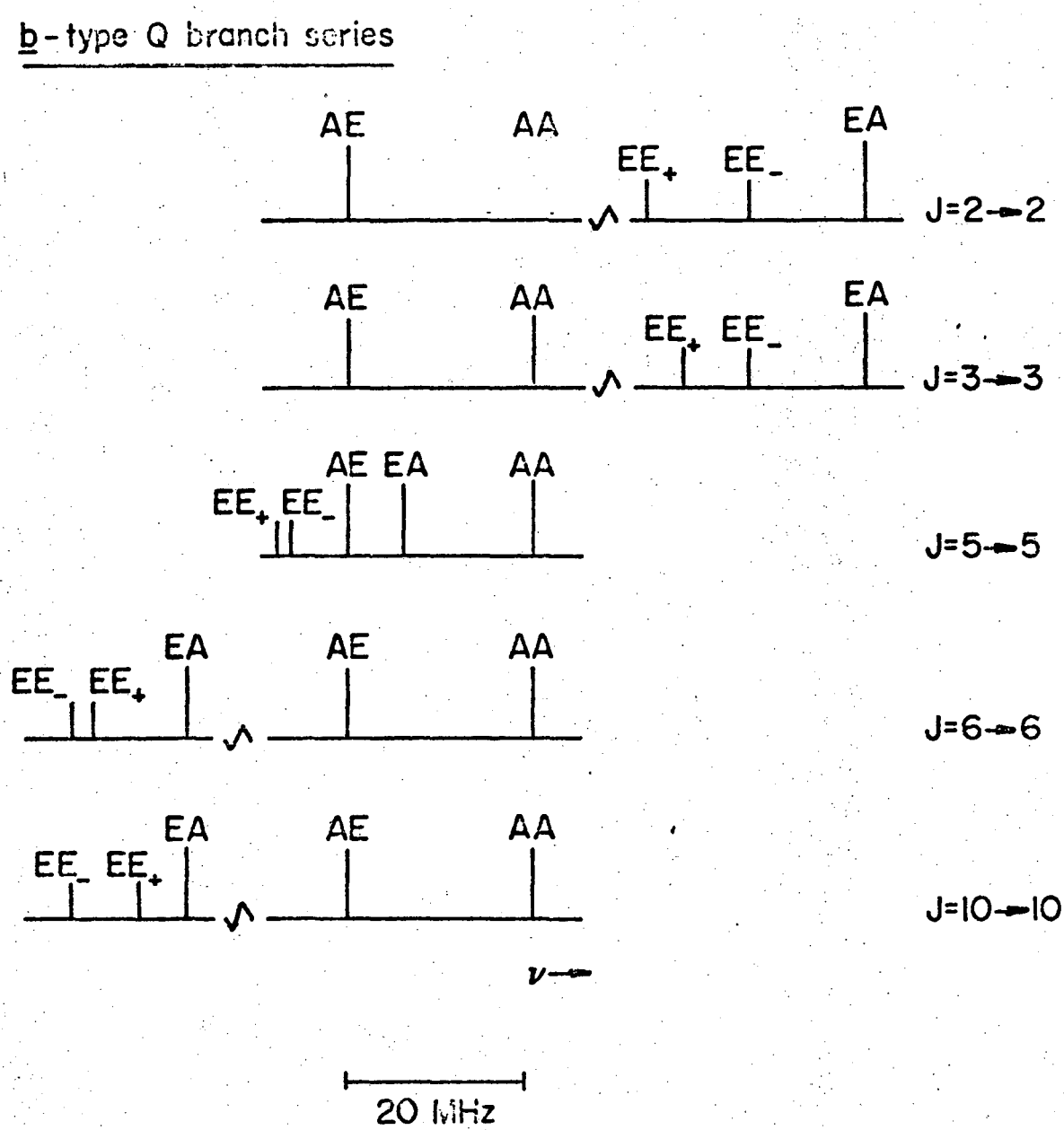

Fig. 4

SiH_3OCH_3

<u>a-type R branch series</u>

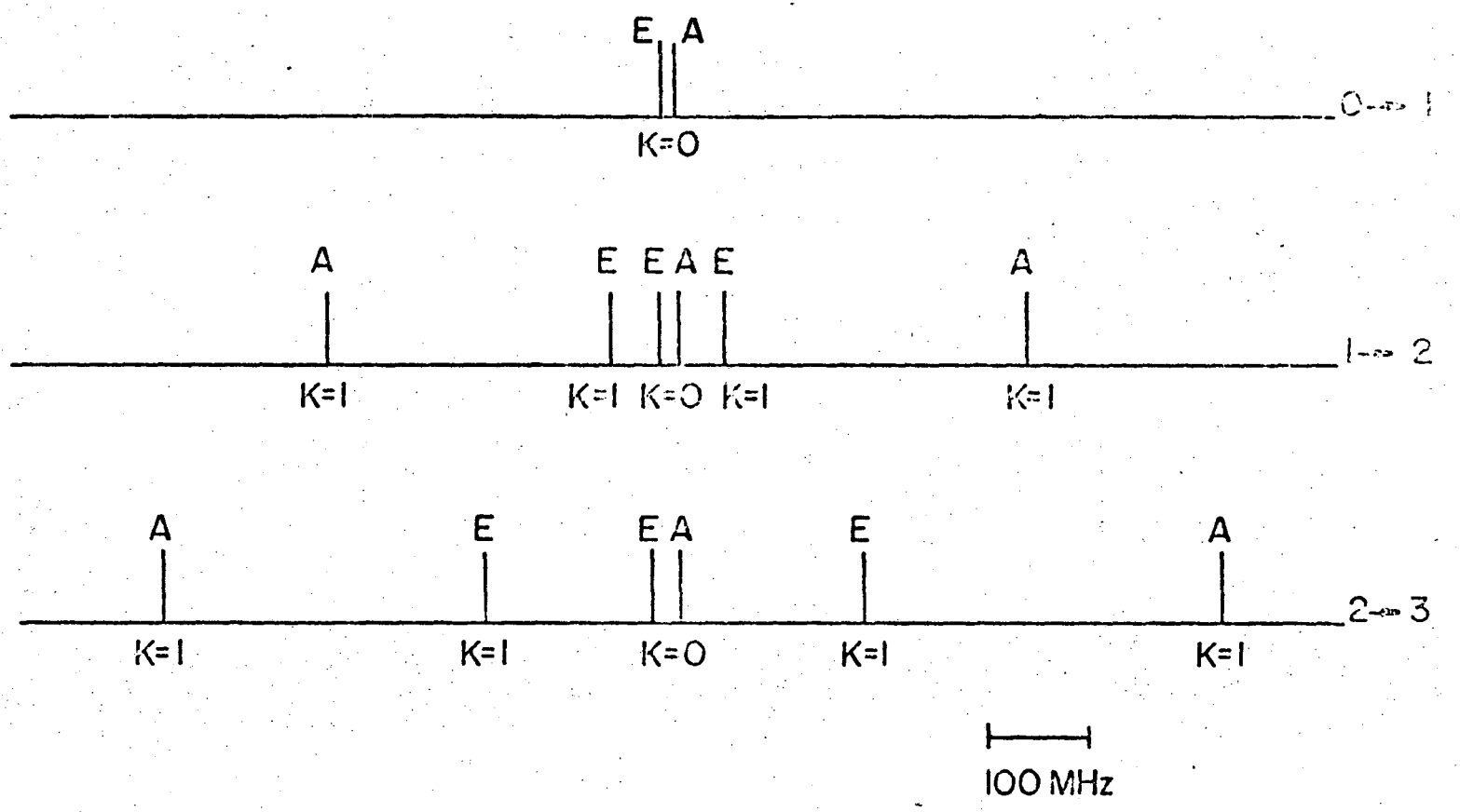

Fig. 5

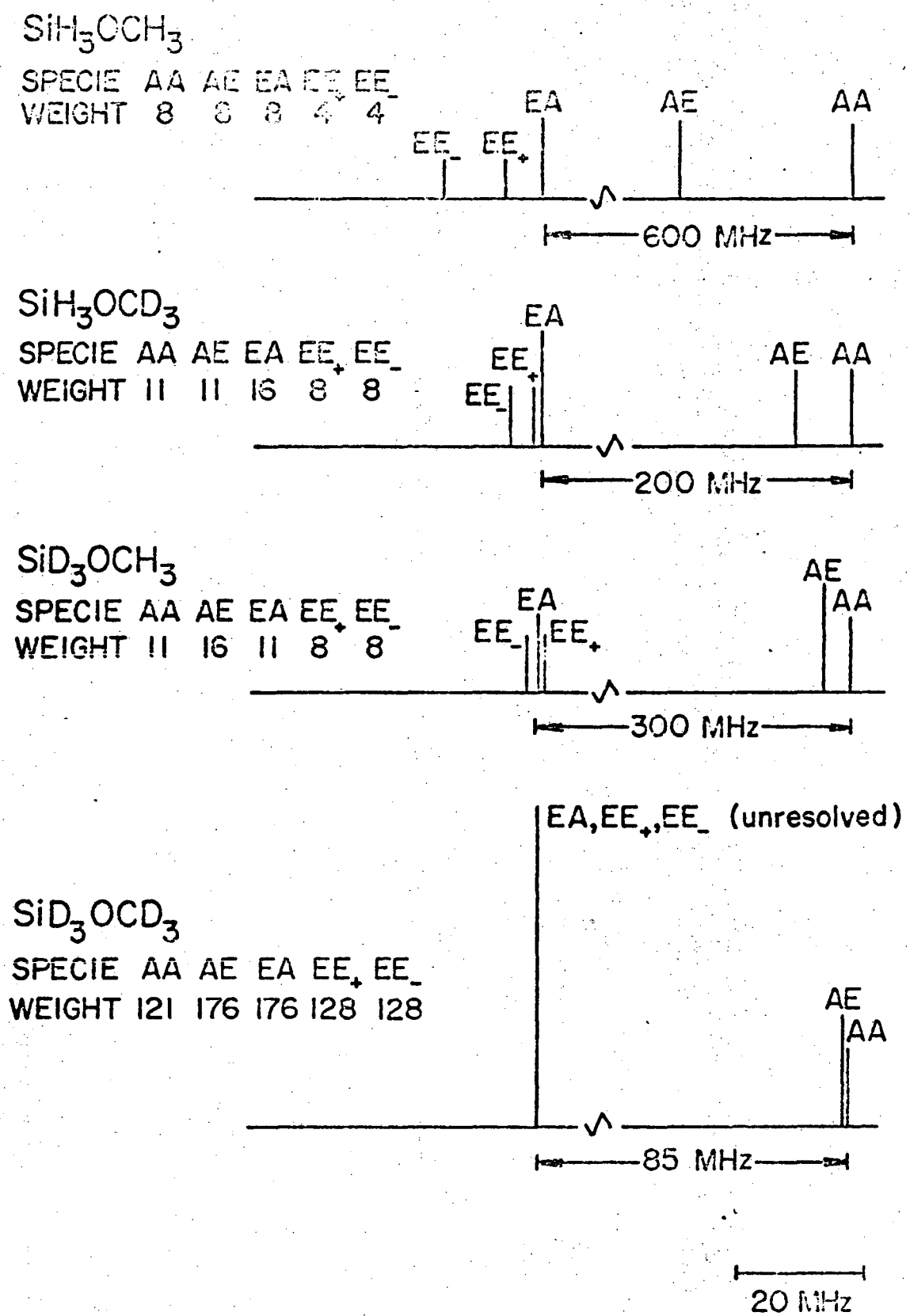
SiH3OCH3
SPECIE AA AE EA EE+ EE-
WEIGHT 8 8 8 4 4
EA
AE
AA
EE-
EE+
600 MHz
SiH3OCD3
SPECIE AA AE EA EE+ EE-
WEIGHT 11 11 16 8 8
EA
EE+
EE-
AE
AA
200 MHz
SiD3OCH3
SPECIE AA AE EA EE+ EE-
WEIGHT 11 16 11 8 8
AE
EA
AA
EE-
EE+
300 MHz
EA,EE+,EE- (unresolved)
SiD3OCD3
SPECIE AA AE EA EE+ EE-
WEIGHT 121 176 176 128 128
AE
AA
85 MHz
20 MHz

Fig. 6

LEGAL NOTICE

This report was prepared as an account of work sponsored by the United States Government. Neither the United States nor the United States Atomic Energy Commission, nor any of their employees, nor any of their contractors, subcontractors, or their employees, makes any warranty, express or implied, or assumes any legal liability or responsibility for the accuracy, completeness or usefulness of any information, apparatus, product or process disclosed, or represents that its use would not infringe privately owned rights.

TECHNICAL INFORMATION DIVISION
LAWRENCE BERKELEY LABORATORY
UNIVERSITY OF CALIFORNIA
BERKELEY, CALIFORNIA 94720